CHAPTER 11

Three-Dimensional Ultrasound in Fetal Atrial, Ventricular and Atrioventricular Septal Defects

Rabih Chaoui*

Prenatal Diagnosis and Human Genetics, Berlin, Germany

Abstract: Atrial, ventricular and atrioventricular septal defects are the most common cardiac anomalies in the humans and occur isolated or as part of other malformations in more than the half of children with a congenital cardiac anomaly. Whereas atrial defects are difficult to detect antenatally, ventricular and atrioventricular defects are detectable on two-dimensional and color Doppler ultrasound. Three-dimensional ultrasound as STIC technology allows in fetal septal defects on one hand a safe description and documentation of the finding and on the other hand a spatial demonstration of the defect with the possibility of getting new views into the heart. The choice of the ideal plane from a 3D volume enables to get the in-line visualization of the interventricular septum with the septal defect. Orthogonal views help to visualize the defect in the different planes. Tomographic imaging aids in getting the upper abdomen and the great vessels information in addition to the septal defect view, in order to rule out a complex malformation. Rendering mode with the enface view can be used to visualize the septum from a lateral view and the common atrioventricular valve in atrioventricular septal defects. The combination with color Doppler helps to get the spatial demonstration of the defect within the heart and provide in addition information on flow events during the cardiac cycle in septal defects.

Key Words: Atrial septal defect, ventricular septal defect, atrioventricular septal defect, Fetal echocardiography, Spatial Temporal Image Correlation, Three-dimensional ultrasound.

DEFINITION

Septal Defects:

A septal defect is an opening of the septum causing communication between the two corresponding chambers, an atrial septal defect (ASD) being a communication between both atria and a ventricular septal defect (VSD) between both ventricles. An atrioventricular septal defect combines a ventricular septal defect with an atrial septum primum defect [1].

Atrial Septal Defects (ASD):

According to its location an ASD is classified into septum primum, septum secundum, sinus venosus and coronary sinus defect, but the most common is in 80% the septum secundum defect also called ASD II.

Ventricular Septal Defects (VSD):

Similarly ventricular septal defects (VSD) are classified according to their location and there are 4 types of VSD: perimembranous, muscular, inlet and outlet. Ventricular septal defects can be isolated or associated with other cardiac defects. Ventricular septal defects associated with conotruncal defects are outlet in location

Atrioventricular Septal Defects (AVSD):

AVSD are classified into partial AVSD which is a synonym of septum primum ASD and into a complete AVSD. In partial AVSD, two distinct mitral and tricuspid valve annuli exist whereas in complete AVSD there is typically an abnormal common atrioventricular valve which connects to the right and left ventricle. The common atrioventricular valve usually has 5 leaflets. Complete AVSD can in addition be classified as balanced or unbalanced. In unbalanced AVSD the atrioventricular connection predominantly drains to one of the two ventricles resulting in ventricular size disproportion.

FETAL SEPTAL DEFECTS ON 2D- AND COLOR DOPPLER ULTRASOUND

Atrial Septal Defect:

It is practically impossible to diagnose reliably an isolated atrial septal defect in the fetus. ASD II is located in the foramen ovale region and it is not possible to predict whether a large foramen ovale will close postnatally or not.

***Address correspondence to Riabih Chaoui:** Prenatal Diagnosis and Human Genetics Friedrichstraße 147; D-10117 Berlin; E-mail: chaoui@feindiagnostik.de

Giuseppe Rizzo and Domenico Arduini (Eds)

ASD I however can be identified in the fetus by the gap in the septum primum region which is generally accompanied with a linear insertion of both atrioventricular valves (Fig. **1**). When combined with other cardiac anomalies the ASD can be suspected.

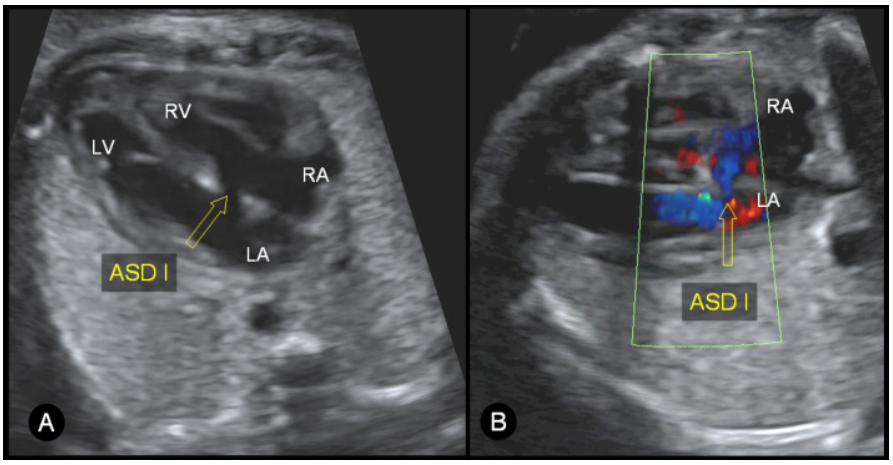

Figure 1: A) Atrial Septum primum defect (ASD I) with the typical gap in the septum primum region (open arrow), B) Color Doppler shows the typical right-to-left shunting (blue) across the ASD-I. LA-left atrium, LV-left ventricle, RA-Right atrium, RV-right ventricle

Color Doppler shows in ASD I a right to left shunt across the defect (Fig. **1**) and blood flow direction is parallel to the alignment of the atrioventricular valves. A left superior vena cava draining into a enlarged coronary sinus may mimic the presence of a ASD I, but in color Doppler the flow in coronary sinus will be opposite.

The detection of an ASD I should alert the examiner to seek for additional cardiac and extracardiac anomalies, especially chromosomal anomalies as trisomy 21 and others.

VENTRICULAR SEPTAL DEFECT (VSD)

This defect can be easily detected on 2D ultrasound when its size is large enough, e.g. larger than 3mm (Fig. **2**).

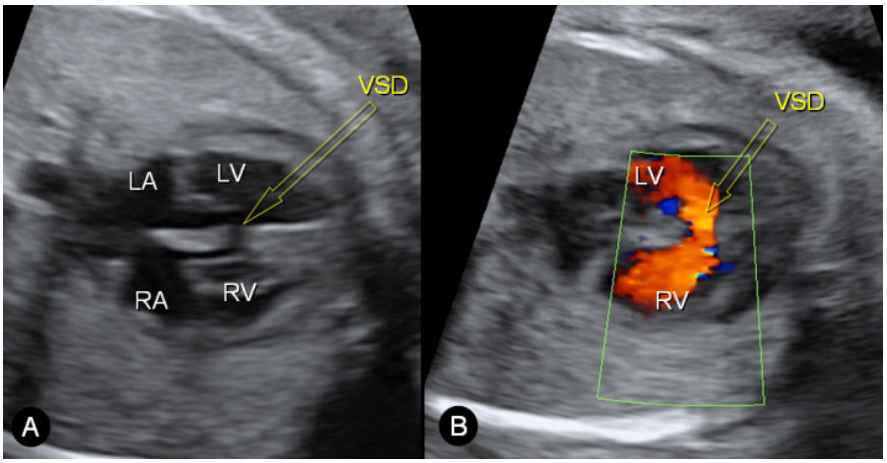

Figure 2: Lateral view of a four-chamber views showing large (>2mm) muscular ventricular septal defect (VSD) in the middle of the septum on 2D (A) and on color Doppler ultrasound (B). LA-left atrium, LV-left ventricle, RA-Right atrium, RV-right ventricle

Smaller VSD need either a targeted examination of the heart or the additional targeted use of color Doppler (Fig. **2**). Most VSD detected prenatally are detected either in a high-risk patient with a positive family history or due to the detection of associated extracardiac anomalies.

An **inlet VSD** is found at the level of the atrioventricular valves in the four-chamber

A **muscular VSD** is generally detected on color Doppler ultrasound and is often found in the apical region of the heart with bidirectional shunt.

A **perimembranous VSD** is detected in the five chamber plane when the continuity between the ventricular septum and the ascending aorta is evaluated. It can be detected on 2D from a lateral view when its size is larger than 2-3 mm but should be confirmed by the presence of bidirectional shunt on color Doppler.

ATRIOVENTRICULAR SEPTAL DEFECT (AVSD)

This anomaly is best detected in the apical four-chamber view either in diastole when the common valve is open presenting the defect in the center of the heart (Fig. **3**) or in systole when the atrioventricular valve is closed presenting the typical linear insertion of both valves. In general a septum primum defect and an inlet ventricular septal defect are recognized in these planes. If the ventricles are of different sizes an unbalanced AVSD should be suspected.

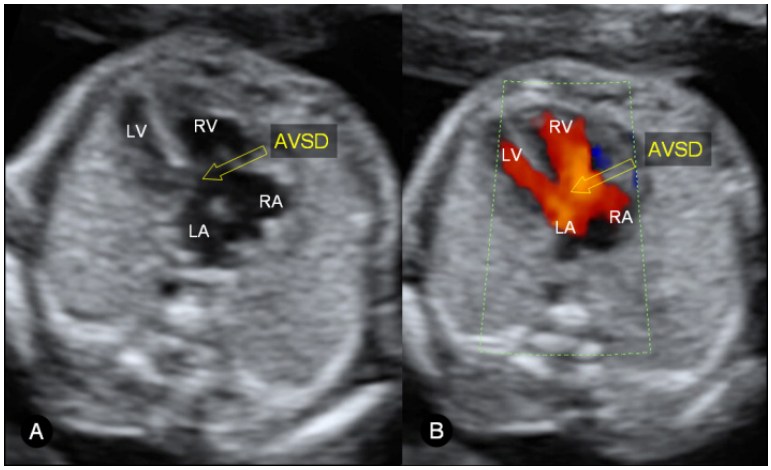

Figure 3: Four-chamber plane in a fetus with complete atrioventricular septal defect (AVSD) visualized during diastole. In A) the arrow points to the gap in the center of the heart. In B) color Doppler shows in diastole how blood flows typically from both atria into both ventricles crossing the midline. LA-left atrium, LV-left ventricle, RA-Right atrium, RV-right ventricle

Color helps to confirm the diagnosis of AVSD showing in diastole blood flow over atrioventricular junction with a mixture of blood of all 4 cavities (Fig. **3**) [2]. In diastole when the valve is closed regurgitation of the common (often dysplastic) atrioventricular valve is found [2].

AVSD is considered as the major cardiac defect found in chromosomal aberrations as trisomy 21, 18 and others. It is also very common in fetuses with heterotaxy syndrome, but in these cases it is not combined with aneuploidies [1]. Once an AVSD is detected the upper abdomen should be carefully examined and the presence of signs of heterotaxy reduce the risk of aneuploidy on one hand but increase the risk of a complex cardiac malformation as part of heterotaxy syndrome on the other.

An easy hint to facilitate detection of an AVSD is the observation of a ratio of atrial-to-ventricular length being more than 0.6 in the majority of cases conversely to a ratio of 0.5 in normal fetuses [3].

THREE-DIMENSIONAL ULTRASOUND IN SEPTAL DEFECTS ORTHOGONAL PLANES AND TOMOGRAPHIC IMAGING

Septal defects are generally small and the information provided by a volume acquired as spatio-temporal image correlation (STIC) is generally superior to a static 3D volume in reliably demonstrating the defect. The demonstration of specific planes of a fetal heart with a septal defect either using 3D orthogonal or tomographic mode, facilitates the visualization of the lesion in addition to its adjacent planes. This visualization provides more information than on conventional 2D sonography. Ventricular and atrioventricular septal defect can be an isolated lesion but can also be a part of a complex cardiac and extracardiac malformation and tomographic ultrasound imaging has been shown to provide a better complete picture of the underlying anomaly in such cases (Figs. **4, 5**) [4].

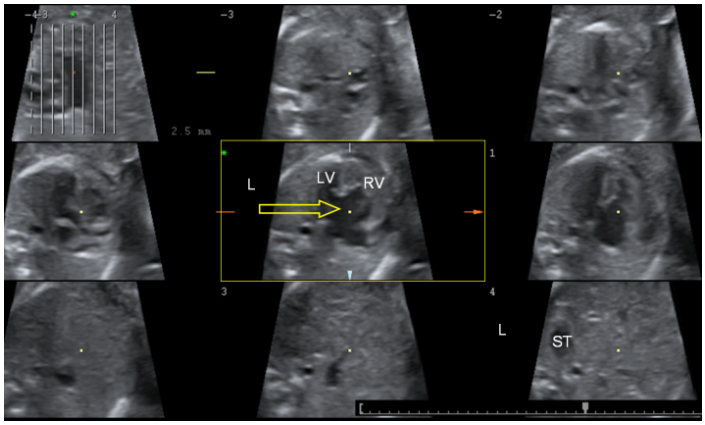

Figure 4: Three dimensional tomographic imaging in a fetus with a detected atrioventricular septal defect (arrow in the middle image). Tomography provides the complete image showing a normal abdominal situs with the stomach (=St) left sided). L-Left. LV-left ventricle, RV-right ventricle

Fig. **4** shows that the AVSD is not associated with heterotaxy, since the stomach is on the left side, whereas Fig. **5** shows the suspected VSD is not an isolated finding but a part of a common arterial trunk.

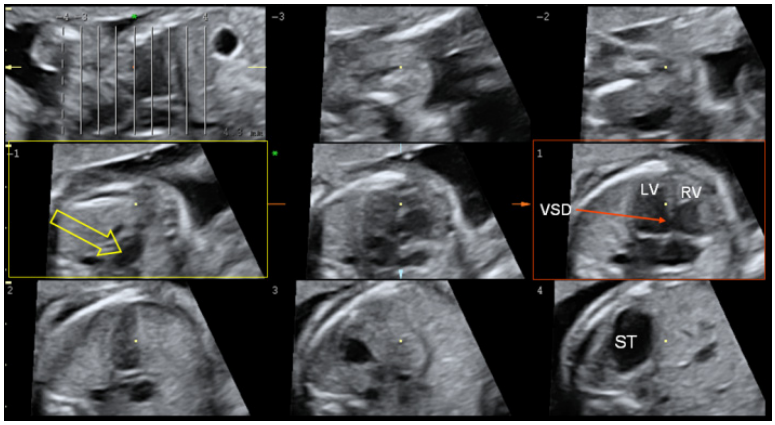

Figure 5: Three dimensional tomographic imaging in a fetus with a detected ventricular septal defect (solid arrow in red box plane). Tomographic imaging provides the additional information of abnormal great vessels (Yellow box). The yellow arrow shows that only one vessel is present. This is not an isolated VSD, but combined with a common arterial trunk. LV-left ventricle, RV-right ventricle

The orthogonal 3D display can be used in gray scale (Fig. **6**) or in combination with color Doppler to demonstrate the presence of a VSD in all three planes, by placing the intersection dot on the shunting VSD (Fig. **6** video 1) [5-6].

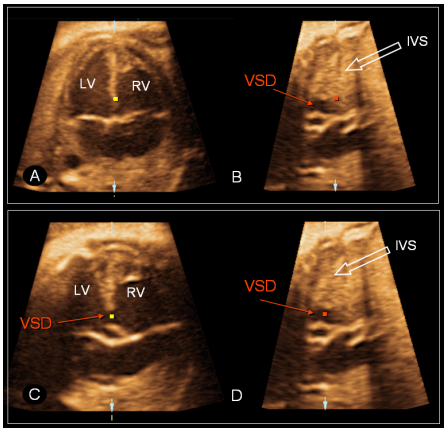

Figure 6: Three-dimensional STIC volume of a heart with a ventricular septal defect (VSD), in orthogonal planes display. In the upper panels A) and B), the apical view A) is shown without the VSD visualized. B) is the orthogonal plane to A) and is the in-

line visualization of the interventricular septum (IVS). In this plane the VSD is recognized red arrow in the perimembranous part of the septum. In C) and D) the intersection dot was moved to be placed in the VSD region in D) and the VSD is also recognized in the apical view in C) as well. RV- right ventricle, LV left ventricle

For AVSD the diagnostic information in small defects is related to the demonstration of diastolic and systolic views, which is facilitated by scrolling through the volume along the time axis of the cardiac cycle (Fig. **7**).

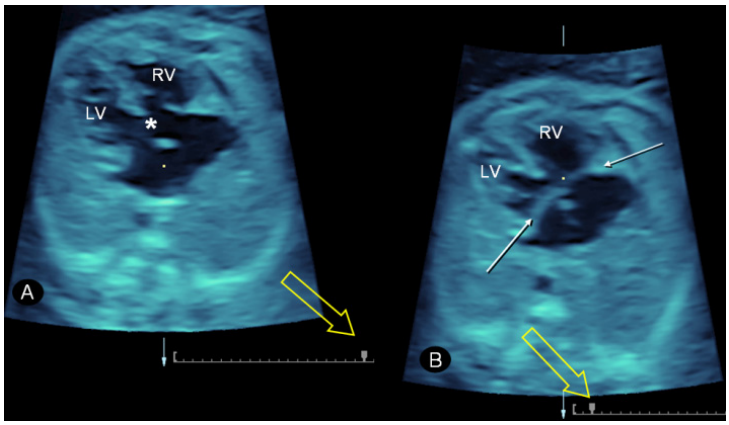

Figure 7: Fetus with atrioventricular (AV) septal defect. Spatio-temporal image correlation allows in addition to the choice of a selective plane (here the apical four-chamber view, the choice of the time within the cardiac cycle (opened arrows on the time axis): In A) diastolic phase with opened AV valve showing the gap in the center of the heart (Asterisk) and in B) systolic phase with closed common AV valve, both valves showing a linear insertion (white arrows). RV- right ventricle, LV left ventricle.

Volume information provides in addition the possibility of getting "ideal planes" or "anyplane" out of a volume [5-6] and the proposed "in-plane" view to demonstrate a septal defect [6], which is a plane along the interventricular septum (see Fig. **6B** and **D**) can be easily retrieved from a STIC volume as shown in Fig. **6**.

SURFACE RENDERING MODE

Surface mode used on gray scale STIC or combined with color Doppler STIC can be used to improve the visualization of septal defects not only in the usual four-chamber view, but also by getting new planes. One of these is the "en face" view of the ventricular septum as shown for the VSD in Fig. **8** and **9**. The study of the ventricular septal defect in this "en-face" view enables for large defects to be better localized on the septum (Fig. **8** perimembranous, and Fig. **9** midmuscular).

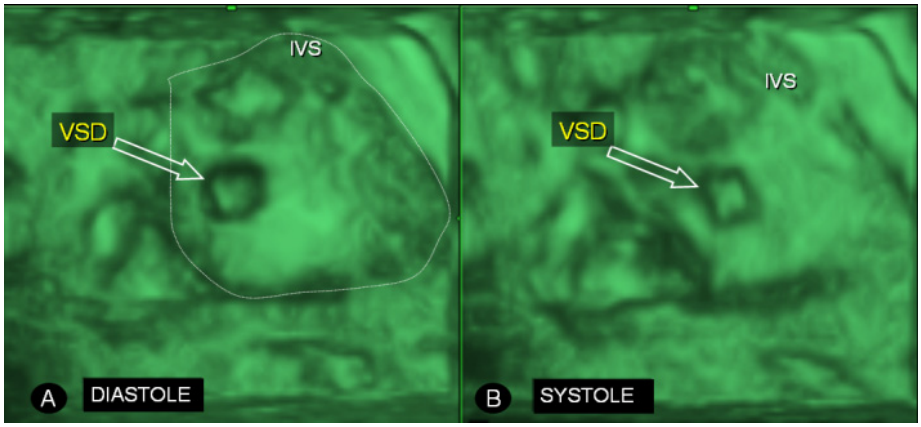

Figure 8: En face view of the interventricular septum (IVS) in a fetus with a large ventricular septal defect (VSD). Both images show clearly how size and shape of the VSD change during the cardiac cycle. In diastole (A) at the maximum of chamber filling the shape is circular and the size is large, whereas in systole when the chamber size is smaller the septum is „squeezed" and the VSD is smaller and the shape not circular anymore.

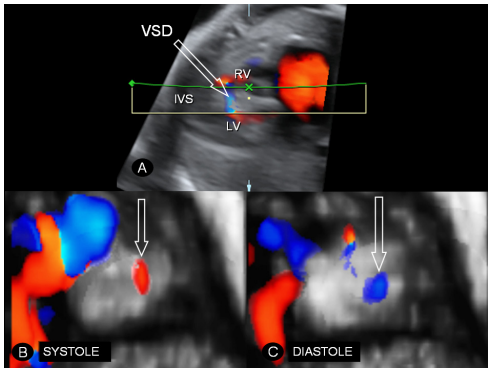

Figure 9: In this fetus with muscular ventricular septal defect (VSD, open arrow) color Doppler STIC acquisition allows the demonstration of flow events across the VSD during the cardiac cycle by using glass-body mode rendering. The rendering box is placed over the interventricular septum (IVS) allowing a view from the right side. During systole (A) blood flow is from left to right (red) and the VSD size appears smaller (compare with previous case). In diastole B) blood flow is from right to left and the VSD size is larger. RV- right ventricle, LV left ventricle

In addition it demonstrates the changes of the size of the defect being large and circular in diastole when chambers are maximally filled with blood and smaller and "squeezed" in systole (Fig. **8** and **9**). The addition of color or power Doppler can be combined with glass body mode to demonstrate either the en-face view on the septum (Fig. **9**) or the anterior view of the heart showing both ventricles connected by the ventricular septal defect and the crossing of great vessels (Fig. **10**).

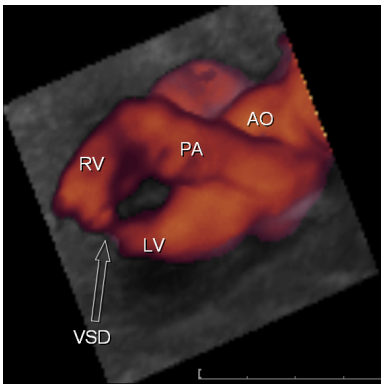

Figure 10: Fetus with a ventricular septal defect (VSD) shown in power Doppler STIC acquisition demonstrating in glass-body mode an anterior view to the heart. Both blood flow in right (RV) and left (LV) ventricles is demonstrated and the crossing of aorta (AO) and main pulmonary artery (PA) are clearly recognized

In atrioventricular septal defects surface rendering at the four-chamber view level may emphasize the size of the gap in the crux of the heart (Fig. **11**. video 2)

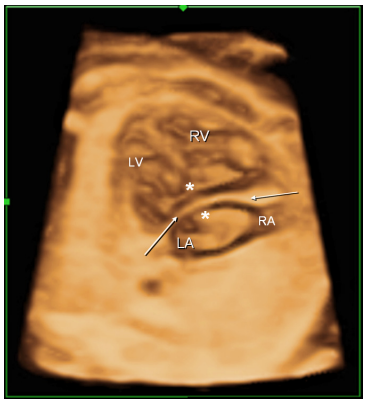

Figure 11: Four-chamber plane of a fetus with atrioventricular septal defect, showing in surface mode rendering of a STIC volume the linear insertion of the common AV valve in systole and the atrial and ventricular septal defects (Asterisks) LA-left atrium, LV-left ventricle, RA-Right atrium, RV-right ventricle

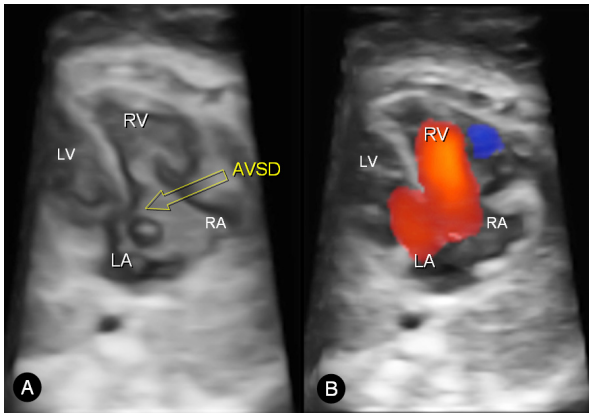

Figure 12: In this fetus with atrioventricular septal defect (AVSD, open arrow) color Doppler STIC acquisition allows the demonstration of flow events across the defect with 3D glass-body mode display A) shows the surface mode rendering during diastole with the opened common valve and B) shows the diastolic filling across the defect (compare with systole in next figure) LA-left atrium, LV-left ventricle, RA-Right atrium, RV-right ventricle

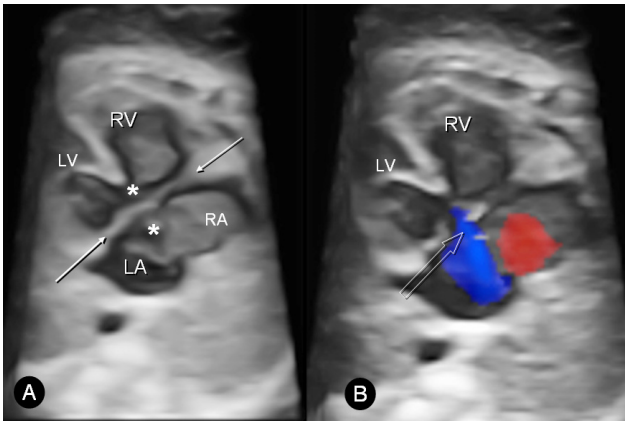

Figure 13: 3D glass-body mode display in a fetus with atrioventricular septal defect showing the four-chamber view during systole. A) surface mode alone shows the defect (asterisks) and the linear insertion of the common AV valve. B) color Doppler added to the surface mode shows the valve regurgitation (open arrow) with blue flow from the ventricle into the atrium. LA-left atrium, LV-left ventricle, RA-Right atrium, RV-right ventricle

The combination of STIC with color Doppler and glass body mode display allows the demonstration of the cardiac cycle related events, namely the mixture of blood flow across the defect during diastole (Fig. **12**) and the valve regurgitation of the common atrioventricular valve during systole (Fig. **13**).

Another approach was proposed to visualize anomalies affecting the atrioventricular valves or the arrangement of the great vessels called the "basic cardiac view" (9) (Fig. **14** video 3)

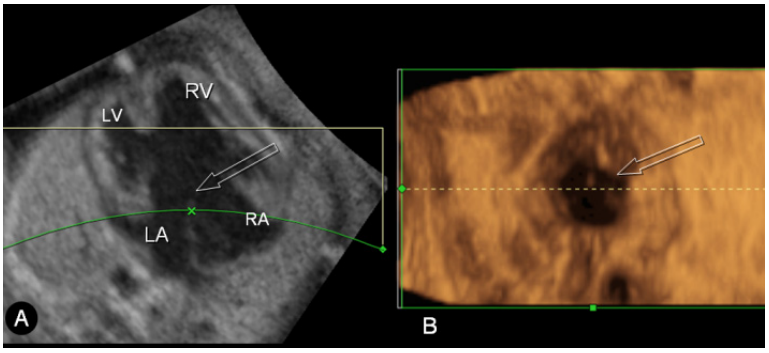

Figure 14: Atrioventricular septal defect (open arrow) with three dimensional surface rendering of STIC volume. The color box is placed in the atria and allows an „en face surface view" on the common valve. In diastole the common valve orifice (B) is demonstrated clearly (open arrow)

When the 3D box is placed within the atria, the en face view on the atrioventricular valves, shows instead of two valves a single opening of the common valve (Fig. **14**). The en-face view of the common AV valve can also be visualized from the ventricles which has in addition the advantage of providing valuable information on the anatomy of the valve apparatus [10].

COLOR DOPPLER, HIGH DEFINITION POWER DOPPLER, INVERSION MODE, B-FLOW RENDERING

The combination of these features with STIC permits the demonstration of flow events across the septal defects as shown before and the rendering mode should be chosen accordingly to the underlying defect and the information wished. The demonstration of flow across a small VSD can for example be shown by combining B-flow or High definition power Doppler with STIC technique both enabling the detection of small defects. The use of inversion mode however, is preferably used for larger defects already recognizable on 2D [11].

CONCLUSIONS

Septal defects in the fetus may be detected on two-dimensional ultrasound but are always confirmed by the use of color Doppler ultrasound. The use of three-dimensional ultrasound in fetal septal defects will preferably use spatio-temporal image correlation (STIC) acquisition. According to the wished information, orthogonal or tomography display modes can provide a better complete picture of the defect with neighbouring structures visualized, as well as an ideal demonstration of site and the range of the defect. Surface mode allows different views either the commonly used transverse views (four-chamber e.g.) or new “en face” views directly on the septum or on the atrioventricular valves. The additional combination of STIC with color Doppler, or other acquisition tools may add the spatial information of flow events in septal defects.

REFERENCES

[1] Esh-Broder E, Ushakov FB, Imbar T, Yagel S. Application of free-hand three-dimensional echocardiography in the evaluation of fetal cardiac ejection fraction: a preliminary study. Ultrasound Obstet Gynecol 2004; 23(6): 546-51.

[2] Simpson JM, Cook A. Repeatability of echocardiographic measurements in the human fetus. Ultrasound Obstet Gynecol 2002; 20(4):332-9.

[3] Teichholz LE, Kreulen T, Herman MV, Gorlin R. Problems in echocardiographic volume determinations: echocardiographic-angiographic correlations in the presence or absence of asynergy. Am J Cardiol 1976; 37(1):7-11.

[4] Bhat AH, Corbett V, Carpenter N, *et al*. Fetal ventricular mass determination on three-dimensional echocardiography: studies in normal fetuses and validation experiments. Circulation 2004; 110(9):1054-60.

[5] Wyatt HL, Meerbaum S, Heng MK, Gueret P, Corday E. Cross-sectional echocardiography. III. Analysis of mathematic models for quantifying volume of symmetric and asymmetric left ventricles. Am Heart J 1980; 100(6 Pt 1):821-8.

[6] Sedmera D, Pexieder T, Vuillemin M, Thompson RP, Anderson RH. Developmental patterning of the myocardium. Anat Rec 2000; 258(4): 319-337.

[7] Simpson J. Echocardiographic evaluation of cardiac function in the fetus. Prenat Diagn 2004; 24 (13): 1081-91.

[8] Bhat AH, Corbett VN, Liu R, *et al.* Validation of volume and mass assessments for human fetal heart imaging by 4-dimensional spatiotemporal image correlation echocardiography: in vitro balloon model experiments. J Ultrasound Med 2004; 23(9)1151-

[9] Espinoza J, Gotsch F, Kusanovic, JP, *et al.* Changes in fetal cardiac geometry with gestation: implications for 3- and 4-dimensional fetal echocardiography. J Ultrasound Med 2007; 26(4): 427-43.

[10] Levental M, Pretorius DH, Sklansky MS, Budorick NE, Nelson TR, Lou K. Three-dimensional ultrasonography of normal fetal heart: comparison with two-dimensional imaging. J Ultrasound Med 1998; 17(6):341-8.

[11] Meyer-Wittkopf M, Cole A, Cooper SG, Schmidt S, Sholler GF. Three-dimensional quantitative echocardiographic assessment of ventricular volume in healthy human fetuses and in fetuses with congenital heart disease. J Ultrasound Med 2001; 20(4):317-27.

12] Tutschek B, Sahn DJ. Semi-automatic segmentation of fetal cardiac cavities: progress towards an automated fetal echocardiogram. Ultrasound Obstet Gynecol 2008; 32(2):176-80.

[13] Uittenbogaard LB, Haak MC, Spreeuwenberg MD, VanVugt JMG. A systematic analysis of the feasibility of four-dimensional ultrasound imaging using spatiotemporal image correlation in routine fetal echocardiography. Ultrasound Obstet Gynecol 2008; 31(6): 625- 32.

[14] Huhta J. Congestive heart failure in the fetus. In Fetal Cardiology (2nd edition), Yagel S, Silverman NH, Gembruch U (eds.). Informa Healthcare USA, Inc: New York, NY, 2009; 561-78.

[15] Messing B, Cohen SM, Valsky DV, *et al*. Fetal cardiac ventricle volumetry in the second half of gestation assessed by 4D ultrasound using STIC combined with inversion mode. Ultrasound Obstet Gynecol 2007; 30(2):142-51.

[16] Molina FS, Faro C, Sotiriadis A, Dagklis T, Nicolaides KH. Heart stroke volume and cardiac output by four-dimensional ultrasound in normal fetuses. Ultrasound Obstet Gynecol 2008; 32(2):181-7.

[17] Rizzo G, Capponi A, Cavicchioni O, Vendola M, Arduini D. Fetal cardiac stroke volume determination by four-dimensional ultrasound with spatio-temporal image correlation compared with two-dimensional and Doppler ultrasonography. Prenat Diagn 2007; 27(12): 1147-50.

[18] Uittenbogaard LB, Haak MC, Spreeuwenberg MD, VanVugt JMG. Fetal cardiac function assessed with four-dimensional ultrasound imaging using spatiotemporal image correlation. Ultrasound Obstet Gynecol 2009; 33(3):272-81.

[19] DeVore GR, Falkensammer P, Sklansky MS, Platt LD. Spatio-temporal image correlation (STIC): new technology for evaluation of the fetal heart. Ultrasound Obstet Gynecol 2003; 22(4):380-7.

20] Gonçalves LF, Lee W, Espinoza J, Romero R. Examination of the fetal heart by four-dimensional (4D) ultrasound with spatio-temporal image correlation (STIC). Ultrasound Obstet Gynecol 2006; 27(3):336-48.

[21] Nelson TR, Pretorius DH, Sklansky M, Hagen-Ansert S. Three-dimensional echocardiographic evaluation of fetal heart anatomy and function: acquisition, analysis, and display. J Ultrasound Med 1996; 15(1):1-9.

[22] Gonçalves LF, Espinoza J, Lee W, Mazor M, Romero R. Three- and four-dimensional reconstruction of the aortic and ductal arches using inversion mode: a new rendering algorithm for visualization of fluid-filled anatomical structures. Ultrasound Obstet Gynecol 2004; 24(6):696-98.

[23] National Institute of Standards and Technology. Guidelines for Evaluating and Expressing the Uncertainty of NIST Measurement Results. http://emtoolbox.nist.gov/Publications/NISTTechnicalNote1297s.pdf (July 13 2009).

[24] Bartlett JW, Frost C. Reliability, repeatability and reproducibility: analysis of measurement errors in continuous variables. Ultrasound Obstet Gynecol 2008; 31(4): 466-75.

[25] Hamill N, Romero R, Hassan S, *et al.* The repeatability and reproducibility of fetal cardiac ventricular volume calculations utilizing Spatio-Temporal Image Correlation (STIC) and Virtual Organ Computer-aided AnaLysis (VOCAL™). J Ultrasound Med, in press.

[26] Mielke G, Benda N. Cardiac output and central distribution of blood flow in the human fetus. Circulation 2001; 103(12)1662-8.

[27] Stewart WJ, Jiang L, Mich R, Pandian N, Guerrero JL, Weyman AE. Variable effects of changes in flow rate through the aortic, pulmonary and mitral valves on valve area and flow velocity: impact on quantitative Doppler flow calculations. J Am Coll Cardiol 1985; 6(3):653-62.

[28] Eik-Nes S, Marsal K, Kristofferson K. Methodology and basic problems related to blood flow studies in the human fetus. Ultrasound Med Biol 1984; 10(3):329-37.

[29] Chaoui R, Heling KS, Taddei F, Bollmann R. Doppler echocardiographic analysis of blood flow through the fetal aorta and pulmonary valve in the second half of pregnancy. Geburt Frauneh 1995; 55(4): 207-17.

[30] Rasanen J, Wood DC, Weiner S, Ludomirski A, Huhta JC. Role of the pulmonary circulation in the distribution of human fetal cardiac output during the second half of pregnancy. Circulation 1996; 94(5): 1068-1073.

[31] Thornburg KL, Reller MD. Coronary flow regulation in the fetal sheep. Am J Physiol 1999; 277(5 Pt 2): R1249-60.

[32] Schmidt KG, Silverman NH, Hoffman JIE. Determination of ventricular volumes in human fetal hearts by two-dimensional echocardiography. Am J Cardiol 1995; 76(17):1313-16.

[33] Allan LD, Chita SK, Al-Ghazali W, Crawford DC, Tynan M. Doppler echocardiographic evaluation of the normal human fetal heart. Br Heart J 1987; 57(6):528-33.

[34] De Smedt MC, Visser GH, Meijboom EJ. Fetal cardiac output estimated by Doppler echocardiography during mid- and late gestation. Am J Cardiol 1987; 60(4):338-42.

[35] Kenny JF, Plappert T, Doubilet P, *et al.* Changes in intracardiac blood flow velocities and right and left ventricular stroke volumes with gestational age in the normal human fetus: a prospective Doppler echocardiographic study. Circulation 1986; 74(6):1208-16.

[36] Veille JC, Sivakoff M, Nemeth M. Evaluation of the human fetal cardiac size and function. Am J Perinatol 1990; 7(1):54-9.

[37] Anderson PAW. Myocardial development. In Fetal and Neonatal Cardiology, Long W (ed.). W.B. Saunders: Philadelphia, PA, 1990; 17-38.

[38] Teitel DF. Physiologic Development of the Cardiovascular System in the Fetus. In Fetal and Neonatal Physiology (3rd edition), Polin RA, Fox WW, Abman H (eds.). W.B. Saunders: Philadelphia, PA, 2003; 609-19.

[39] Winberg P, Jansson M, Marions L, Lundell BP. Left ventricular output during postnatal circulatory adaptation in healthy infants born at full term. Arch Dis Child 1989; 64:1374-78.

[40] Pemberton J, Li X, Kenny A, Davies CH, Minette MS, Sahn DJ. Real-time 3-dimensional Doppler echocardiography for the assessment of stroke volume: an in vivo human study compared with standard 2-dimensional echocardiography. J Am Soc Echocardiogr 2005; 18(10):1030-36.